

Charmed Hadron Asymmetries in the Intrinsic Charm  
Coalescence Model \*

R. Vogt

Nuclear Science Division  
Lawrence Berkeley Laboratory  
Berkeley, California 94720  
andPhysics Department  
University of California at Davis  
Davis, California 95616

and

S. J. Brodsky

Stanford Linear Accelerator Center  
Stanford University  
Stanford, California 94309

(Submitted to Nuclear Physics B.)

---

\* This work was supported in part by the Director, Office of Energy Research, Division of Nuclear Physics of the Office of High Energy and Nuclear Physics of the U. S. Department of Energy under Contract Numbers DE-AC03-76SF0098 and DE-AC03-76SF00515.

## ABSTRACT

Fermilab experiment E791, measuring charmed hadron production in  $\pi^- A$  interactions at 500 GeV with high statistics, has observed a strong asymmetry between the hadroproduction cross sections for leading  $D$  mesons which contain projectile valence quarks and the nonleading charmed mesons without projectile valence quarks. Such correlations of the charge of the  $D$  meson with the quantum numbers of the beam hadron explicitly contradict the factorization theorem in perturbative QCD which predicts that heavy quarks hadronize through a jet fragmentation function that is independent of the initial state. The E791 experiment also measures  $\Lambda_c/\overline{\Lambda}_c$  and  $D_s/\overline{D}_s$  production asymmetries as well as asymmetries in  $D\overline{D}$  pair production. We examine these asymmetries and the fractional longitudinal momentum,  $x_F$ , distributions for single and pairs of charmed hadrons within a two-component model combining leading-twist  $gg$  and  $q\overline{q}$  fusion subprocesses with charm production from intrinsic heavy quark Fock states. A key feature of this analysis is intrinsic charm coalescence, the process by which a charmed quark in the projectile's Fock state wavefunction forms charmed hadrons by combining with valence quarks of similar rapidities.

## 1. Introduction

The E791 experiment, studying 500 GeV  $\pi^- A$  interactions with carbon and platinum targets, employs an open geometry spectrometer with a very open trigger and a fast data acquisition system to record the world's largest sample of hadroproduced charm [1]. This large data set allows detailed investigations of charmed hadron production including  $\Lambda_c(udc)$ ,  $\bar{\Lambda}_c$ ,  $D_s(c\bar{s})$ ,  $\bar{D}_s$ , and  $D\bar{D}$  pairs.

One of the most striking features of charm hadroproduction is the leading particle effect: the strong correlation between the quantum number of the incident hadron and the quantum numbers of the final-state charmed hadron. For example, more  $D^-$  than  $D^+$  are produced at large  $x_F$  in  $\pi^- A \rightarrow D^\pm X$  [1, 2, 3, 4, 5]. There is also evidence of leading particle correlations in  $\Lambda_c$  [6, 7, 8] and  $\Lambda_b(udb)$  [9] production in  $pp$  collisions and  $\Xi_c(usc)$  production in hyperon-nucleon interactions [10, 11]. Such correlations are remarkable because they explicitly contradict the factorization theorem in perturbative QCD which predicts that heavy quarks hadronize through a jet fragmentation function that is independent of the initial state.

Leading charm production can be quantified by studies of the production asymmetries between leading and nonleading charm production. In  $\pi^- p$  interactions, both  $D^-(\bar{c}d)$  and  $D^0(c\bar{u})$ , which share valence quarks with the  $\pi^-(\bar{u}d)$ , are “leading” while  $D^+(c\bar{d})$  and  $\bar{D}^0(\bar{c}u)$ , which do not, are “nonleading” at  $x_F > 0$ . The harder leading  $D$  distributions suggest that hadronization at large  $x_F$  involves the recombination of the charmed or anticharmed quarks with the projectile spectator valence quarks. The  $D^-/D^+$  asymmetry is defined as

$$\mathcal{A}_{D^-/D^+} = \frac{d\sigma(D^-) - d\sigma(D^+)}{d\sigma(D^-) + d\sigma(D^+)} . \quad (1)$$

The measured asymmetry increases from nearly zero at small  $x_F$  to  $\mathcal{A}_{D^-/D^+} \sim 0.5$  around  $x_F = 0.65$  [4, 5], indicating that the leading charm asymmetry is primarily localized at large  $x_F$ . Thus the asymmetry  $\mathcal{A}_{D^-/D^+}$  reflects the physics of only a small fraction of the total  $D^\pm$  cross section. The neutral  $D$ 's were not used in the

analysis since these states can also be produced indirectly by the decay of nonleading  $D^{*+}$  mesons.

In a recent paper [12], we discussed a QCD mechanism which produces a strong asymmetry between leading and nonleading charm at large  $x_F$ . A key feature of this analysis is coalescence, the process by which a produced charmed quark forms charmed hadrons by combining with quarks of similar rapidities. In leading-twist QCD, heavy quarks are produced by the fusion subprocesses  $gg \rightarrow Q\bar{Q}$  and  $q\bar{q} \rightarrow Q\bar{Q}$ . The factorization theorem [13] predicts that fragmentation is independent of the quantum numbers of both the projectile and target. Thus one expects  $\mathcal{A} = 0$  to leading order. However, it is possible that the forward-moving heavy quarks will coalesce with the spectator valence quarks of the projectile to produce leading hadrons in the final state. In a gauge theory one expects the strongest attraction to occur when the spectator and produced quarks have equal velocities [14]. Thus the coalescence probability should be largest at small relative rapidity and relatively low transverse momentum where the invariant mass of the  $\bar{Q}q$  system is minimal, and its amplitude for binding is maximal.

The coalescence of charmed quarks with projectile valence quarks may also occur in the initial state. For example, the  $\pi^-$  or  $p$  wavefunctions can fluctuate into  $|\bar{u}dc\bar{c}\rangle$  or  $|uudc\bar{c}\rangle$  Fock states. These states are produced in QCD from amplitudes involving two or more gluons attached to the charmed quarks. The most important fluctuations occur at minimum invariant mass  $M$  where all the partons have approximately the same velocity. These fluctuations can have very long lifetimes in the target rest frame,  $\mathcal{O}(2P_{\text{lab}}/M^2)$ , where  $P_{\text{lab}}$  is the projectile momentum. Since the charm and valence quarks have the same rapidity in these states, the heavy quarks carry a large fraction of the projectile momentum. Furthermore the comoving heavy and light quarks can readily coalesce to produce leading charm correlations at a large combined longitudinal momentum. Such a mechanism can dominate the hadroproduction rate at large  $x_F$ . This is the underlying assumption of the intrinsic charm model [15].

The intrinsic charm fluctuations in the wavefunction are initially far off the light-cone energy shell. However, they become on shell and materialize into charmed hadron when a light spectator quark in the projectile Fock state interacts in the target [16]. Since such interactions are strong, the charm production will occur primarily on the front face of the nucleus in the case of a nuclear target. Thus an important characteristic of the intrinsic charm model is its strong nuclear dependence; the cross section for charm production via the materialization of heavy Fock states should have a nuclear dependence at high energies similar to that of inelastic hadron-nucleus cross sections.

In this work, we concentrate on the charmed hadrons and meson pairs channels studied by E791 in order to further examine the relationship between fragmentation and coalescence mechanisms. The calculations are made within a two-component model: leading-twist fusion and intrinsic charm [12, 17, 18]. We find that the coalescence of the intrinsic charmed quarks with the valence quarks of the projectile is the dominant mechanism for producing fast  $D$  and  $D^*$  mesons. On the other hand, when the charmed quarks coalesce with sea quarks, there is no leading charmed hadron. We discuss the longitudinal momentum distributions and the related asymmetries for  $\Lambda_c/\overline{\Lambda}_c$  and  $D_s/\overline{D}_s$  production, as well as  $D\overline{D}$  pairs. (We have only applied our model to  $D\overline{D}$  pairs in the forward hemisphere in order to provide a clear definition of the asymmetry.)

As expected, the asymmetries predicted by the intrinsic charm coalescence model are a strong function of  $x_F$ . We find that  $\Lambda_c$  production in the proton fragmentation region ( $x_F < 0$  in  $\pi^-p$  collisions) is dominated by the coalescence of the intrinsic charm quark with the  $ud$  valence quarks of the proton. Coalescence is particularly important in  $D\overline{D}$  pair production. The production of  $D_s/\overline{D}_s$  and, at  $x_F > 0$ ,  $\Lambda_c/\overline{\Lambda}_c$  by coalescence must occur within still higher particle number Fock states.

Leading particle correlations are also an integral part of the Monte Carlo program PYTHIA [19] based on the Lund string fragmentation model. In this model it is

assumed that the heavy quarks are produced in the initial state with relatively small longitudinal momentum fractions by the leading twist fusion processes. In order to produce a strong leading particle effect at large  $x_F$ , the string has to accelerate the heavy quark as it fragments and forms the final-state heavy hadron. Such a mechanism goes well beyond the usual assumptions made in hadronization models and arguments based on heavy quark symmetry, since it demands that large changes of the heavy quark momentum take place in the final state.

In this paper we shall compare the predictions of the intrinsic charm coalescence model with those of PYTHIA [19]. The comparison of the data with these models should distinguish the importance of higher heavy quark Fock state fluctuations in the initial state and the coalescence process from the strong string hadronization effects postulated in the PYTHIA model.

## 2. Leading-Twist Production

In this section we briefly review the conventional leading-twist model for the production of single charmed hadrons and  $D\bar{D}$  pairs in  $\pi^-p$  interactions. We will also show the corresponding distributions of charmed hadrons predicted by the PYTHIA model [19].

Our calculations are at lowest order in  $\alpha_s$ . A constant factor  $K \sim 2-3$  is included in the fusion cross section since the next-to-leading order  $x_F$  distribution is larger than the leading order distribution by an approximately constant factor [20]. Neither leading order production nor the next-to-leading order corrections can produce flavor correlations [21].

The single charmed hadron  $x_F$  distribution,  $x_F = (2m_T/\sqrt{s}) \sinh y$ , has the factorized form [18]

$$\frac{d\sigma}{dx_F} = \frac{\sqrt{s}}{2} \int H_{ab}(x_a, x_b) \frac{1}{E_1} \frac{D_{H/c}(z_3)}{z_3} dz_3 dy_2 dp_T^2, \quad (2)$$

where  $a$  and  $b$  are the initial partons, 1 and 2 are the charmed quarks with  $m_c = 1.5$  GeV, and 3 and 4 are the charmed hadrons. The convolution of the subprocess cross sections for  $q\bar{q}$  annihilation and gluon fusion with the parton densities is included in  $H_{ab}(x_a, x_b)$ ,

$$H_{ab}(x_a, x_b) = \sum_q [f_q^A(x_a) f_{\bar{q}}^B(x_b) + f_{\bar{q}}^A(x_a) f_q^B(x_b)] \frac{d\hat{\sigma}_{q\bar{q}}}{d\hat{t}} + f_g^A(x_a) f_g^B(x_b) \frac{d\hat{\sigma}_{gg}}{d\hat{t}}, \quad (3)$$

where  $A$  and  $B$  are the interacting hadrons. For consistency with the leading-order calculation, we use current leading order parton distribution functions, GRV LO, for both the nucleon [22] and the pion [23].

The fragmentation functions,  $D_{H/c}(z)$ , describe the hadronization of the charmed quark where  $z = x_H/x_c$  is the fraction of the charmed quark momentum carried by the charmed hadron, produced roughly collinear to the charmed quark. Assuming factorization, the fragmentation is independent of the initial state (leptons or hadrons) and thus cannot produce flavor correlations between the projectile valence quarks and the charmed hadrons. This uncorrelated fragmentation will be modeled by two extremes: a delta function,  $\delta(z-1)$ , and the Peterson function [24], as extracted from  $e^+e^-$  data. The Peterson function predicts a softer  $x_F$  distribution than observed in hadroproduction, even at moderate  $x_F$  [18], since the fragmentation decelerates the charmed quark, decreasing its average momentum fraction,  $\langle x_F \rangle$ , approximately 30% by the production of  $D$  mesons. The delta-function model assumes that the charmed quark coalesces with a low- $x$  spectator sea quark or a low momentum secondary quark such that the charmed quark retains its momentum [18]. This model is more consistent with low  $p_T$  charmed hadroproduction data [25, 26, 27] than Peterson fragmentation.

The parameters of the Peterson function we use here are taken from  $e^+e^-$  studies of  $D$  production [28]. The  $D^*$  distributions are very similar to the  $D$  distributions but the  $\Lambda_c$  distribution appears to be somewhat softer [29]. Although there is some uncertainty in the exact form of the Peterson function for charmed baryons and  $D_s$  mesons, it always produces deceleration.

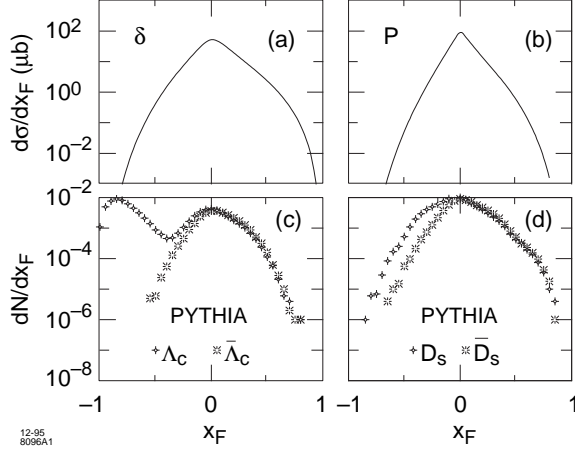


Figure 1: Leading-twist fusion calculations of single charm production from  $\pi^-p$  interactions at 500 GeV with delta function (a) and Peterson function (b) fragmentation. The results from the PYTHIA Monte Carlo [19] for  $\Lambda_c/\bar{\Lambda}_c$  (c) and  $D_s/\bar{D}_s$  (d) production are also shown. The fusion calculations are normalized to the charm cross section while the PYTHIA distributions are normalized to the number per event.

In Fig. 1 we show the single inclusive  $x_F$  distributions calculated for (a) delta function and (b) Peterson function fragmentation in  $\pi^-p$  interactions at 500 GeV. The results are normalized to the total single charmed quark cross section. The parton distributions of the pion are harder than those of the proton at large  $x_{Bj}$ , producing broader forward distributions. As expected, the delta-function fragmentation results in harder distributions than those predicted by Peterson fragmentation for  $x_F > 0.2$ . However, as shown in [4], the conventional fusion model, even with delta-function fragmentation, cannot account for the shape of leading  $D$  distributions.

The charmed hadron distributions from PYTHIA, obtained from a  $\pi^-p$  run with  $10^6$  events at 500 GeV using all default settings and the GRV LO parton distributions, are shown in Fig. 1(c) for  $\Lambda_c$  and  $\bar{\Lambda}_c$  and 1(d) for  $D_s$  and  $\bar{D}_s$  hadrons. The distributions are normalized to the number of charmed hadrons per event. PYTHIA is based on the Lund string fragmentation model [19] in which charmed quarks are at string endpoints. The strings pull the charmed quarks toward the opposite string endpoints, usually beam remnants. When the two string endpoints are moving in the



same general direction, the charmed hadron can be produced with larger longitudinal momentum than the charmed quark, accelerating it. In the extreme case where the string invariant mass is too small to allow multiple particle production, this picture reduces to final-state coalescence and the string endpoints determine the energy, mass, and flavor content of the produced hadron [30]. Thus a  $D^-$  or  $D^0$  can inherit all of the remaining projectile momentum while  $D^+$  and  $\overline{D}^0$  production is forbidden. The coalescence of a charmed quark with a valence diquark results in the secondary peak at  $x_F \approx -0.85$  in the  $\Lambda_c$  distribution shown in Fig. 1(c). The  $\Lambda_c$  baryon is a leading charmed hadron in the proton fragmentation region since it can have two valence quarks in common with the proton. Also in the proton fragmentation region, the  $D_s$  is somewhat harder than the  $\overline{D}_s$ . This is evidently a secondary effect of  $\Lambda(uds)$  coalescence with a  $ud$  diquark: the  $\overline{s}$  can pull the charmed quark to larger  $x_F$  in the wake of the  $\Lambda$ , producing more  $D_s$  at negative  $x_F$  than  $\overline{D}_s$ . Such coalescence correlations are not predicted for the  $\overline{\Lambda}_c$  or the  $\overline{D}_s$  in the proton fragmentation region. In the pion fragmentation region, the predicted  $D_s/\overline{D}_s$  distributions are harder than the  $\Lambda_c/\overline{\Lambda}_c$  distributions.

The charmed pair  $x_F$  distribution is

$$\begin{aligned} \frac{d\sigma}{dx_F} = & \int H_{ab}(x_a, x_b) \frac{E_3 E_4}{E_1 E_2} \frac{D_{H/c}(z_3) D_{\overline{H}/\overline{c}}(z_4)}{z_3 z_4} \delta(M_{D\overline{D}}^2 - 2m_T^2(1 + \cosh(y_3 - y_4))) \\ & \times \delta(x_F - x_3 - x_4) dz_3 dz_4 dy_3 dy_4 dp_T^2 dM_{D\overline{D}}^2, \end{aligned} \quad (4)$$

where  $x_F = x_3 + x_4$  and  $m_T^2 = p_T^2 + m_D^2$ . Figure 2 shows the forward  $x_F$  distribution of  $D\overline{D}$  pairs from  $\pi^- p$  interactions at 500 GeV with (a) delta function and (b) Peterson function fragmentation for both charmed quarks. The distributions are normalized to the total  $c\overline{c}$  pair production cross section. Note that the pair distributions are harder than the single distributions in Fig. 1. The perturbative QCD calculation cannot distinguish between leading and nonleading hadrons in the pair distributions.

In Fig. 2(c), the  $D\overline{D}$  pair distributions from PYTHIA have been classified as doubly leading ( $LL$ ),  $D^- D^0$ , nonleading-leading ( $NL$ ),  $D^- D^+ + D^0 \overline{D}^0$ , and doubly

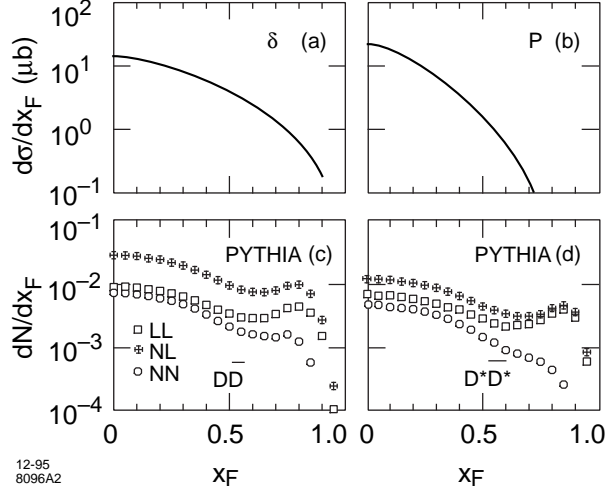


Figure 2: Leading-twist fusion calculations of  $c\bar{c}$  pair production from  $\pi^-p$  interactions at 500 GeV with delta function (a) and Peterson function (b) fragmentation. The results from the PYTHIA Monte Carlo [19] for  $LL$ ,  $NL$ , and  $NN$   $D\bar{D}$  (c) and  $D^*\bar{D}^*$  (d) pairs are also shown. The fusion calculations are normalized to the  $c\bar{c}$  cross section while the PYTHIA distributions are normalized to the number per event.

nonleading ( $NN$ ),  $D^+\bar{D}^0$ . The same classification for  $D^*$  pairs is shown in Fig. 2(d). The distributions are normalized to the number of charmed pairs per event. We have not considered  $D\bar{D}^*$  or  $D^*\bar{D}$  pairs. Note that the leading particle assignments are only valid for  $x_F > 0$ . The assignments are more meaningful for the  $D^*$ 's since they may be assumed to be directly produced. The neutral  $D$  mesons in Fig. 2(c) arise in part from charged  $D^*$  decays. Thus the  $NN$   $D$  pair distributions have a shoulder at  $x_F \approx 0.8$  from  $D^{*-}$  decays to  $\bar{D}^0$  which is absent in the  $NN$   $D^*\bar{D}^*$  distributions. Note also that the  $NL$  pairs are most numerous since both charged and neutral  $D$  pairs contribute to the distribution. Almost three times as many neutral  $D$ 's are produced than charged  $D$ 's. Only some of this difference can arise from  $D^*$  decays since charged and neutral  $D^*$ 's are produced in nearly equal abundance.

Other final-state coalescence models have been proposed, including a valence spectator recombination model [31] and the valon model [32]. Two important unknowns in these models are the correlation between the charmed quark and the valence spec-

tator in the recombination function and the  $n$ -particle parton distributions of the spectator and participant valence quarks. In this work we will not compare to either of these models but simply note that they can also produce charmed hadrons and hadron pairs by final-state coalescence.

### 3. Intrinsic Heavy Quark Production

The wavefunction of a hadron in QCD can be represented as a superposition of Fock state fluctuations, *e.g.*  $|n_V\rangle$ ,  $|n_V g\rangle$ ,  $|n_V Q\bar{Q}\rangle$ , ... components where  $n_V \equiv \bar{u}d$  for a  $\pi^-$  and  $uud$  for a proton. When the projectile scatters in the target, the coherence of the Fock components is broken and the fluctuations can hadronize either by uncorrelated fragmentation or coalescence with spectator quarks in the wavefunction [15, 16]. The intrinsic heavy quark Fock components are generated by virtual interactions such as  $gg \rightarrow Q\bar{Q}$  where the gluons couple to two or more projectile valence quarks. The probability to produce  $Q\bar{Q}$  fluctuations scales as  $\alpha_s^2(m_{Q\bar{Q}})/m_Q^2$  relative to leading-twist production [33] and is thus higher twist. Intrinsic  $Q\bar{Q}$  Fock components are dominated by configurations with equal rapidity constituents so that, unlike sea quarks generated from a single parton, the intrinsic heavy quarks carry a large fraction of the parent momentum [15].

The frame-independent probability distribution of an  $n$ -particle  $c\bar{c}$  Fock state is

$$\frac{dP_{\text{ic}}}{dx_i \cdots dx_n} = N_n \alpha_s^4(M_{c\bar{c}}) \frac{\delta(1 - \sum_{i=1}^n x_i)}{(m_h^2 - \sum_{i=1}^n (\widehat{m}_i^2/x_i))^2} , \quad (5)$$

where  $N_n$ , assumed to be slowly varying, normalizes the  $|n_V c\bar{c}\rangle$  probability,  $P_{\text{ic}}$ . The delta function conserves longitudinal momentum. The dominant Fock configurations are closest to the light-cone energy shell and therefore have minimal invariant mass,  $M^2 = \sum_i \widehat{m}_i^2/x_i$ , where  $\widehat{m}_i^2 = k_{T,i}^2 + m_i^2$  is the effective transverse mass of the  $i^{\text{th}}$  particle and  $x_i$  is the light-cone momentum fraction. Assuming  $\langle \vec{k}_{T,i}^2 \rangle$  is proportional

to the square of the constituent quark mass, we adopt the effective values  $\widehat{m}_q = 0.45$  GeV,  $\widehat{m}_s = 0.71$  GeV, and  $\widehat{m}_c = 1.8$  GeV [17, 18].

The intrinsic charm production cross section can be related to  $P_{\text{ic}}$  and the inelastic  $hN$  cross section by

$$\sigma_{\text{ic}}(hN) = P_{\text{ic}} \sigma_{hN}^{\text{in}} \frac{\mu^2}{4\widehat{m}_c^2} . \quad (6)$$

The factor of  $\mu^2/4\widehat{m}_c^2$  arises because a soft interaction is needed to break the coherence of the Fock state. The NA3 collaboration [34] separated the nuclear dependence of  $J/\psi$  production in  $\pi^-A$  interactions into a “hard” contribution with a nearly linear  $A$  dependence at low  $x_F$  and a high  $x_F$  “diffractive” contribution scaling as  $A^{0.77}$ , characteristic of soft interactions. One can fix the soft interaction scale parameter,  $\mu^2 \sim 0.2$  GeV<sup>2</sup>, by the assumption that the diffractive fraction of the total production cross section [34] is the same for charmonium and charmed hadrons. Therefore, we obtain  $\sigma_{\text{ic}}(\pi N) \approx 0.5$   $\mu\text{b}$  at 200 GeV and  $\sigma_{\text{ic}}(pN) \approx 0.7$   $\mu\text{b}$  [12] with  $P_{\text{ic}} = 0.3\%$  from an analysis of the EMC charm structure function data [35]. A recent reanalysis of this data with next-to-leading order calculations of leading twist and intrinsic charm electroproduction confirms the presence of an  $\approx 1\%$  intrinsic charm component in the proton for large  $x_{\text{Bj}}$  [36]. Note that a larger  $P_{\text{ic}}$  would not necessarily lead to a larger  $\sigma_{\text{ic}}$ . Since we have fixed  $\mu^2$  from the NA3 data, increasing  $P_{\text{ic}}$  would decrease  $\mu^2$  accordingly.

We now calculate the probability distributions,  $dP_{\text{ic}}/dx_F$  for charmed hadrons and  $D\overline{D}$  pairs resulting from both uncorrelated fragmentation and coalescence of the quarks in the intrinsic charmed Fock states. These light-cone distributions are frame independent. In a hadronic interaction, these states are dissociated and materialize with the corresponding differential cross section

$$\frac{d\sigma_{\text{ic}}(hN)}{dx_F} = \sigma_{hN}^{\text{in}} \frac{\mu^2}{4\widehat{m}_c^2} \frac{dP_{\text{ic}}}{dx_F} . \quad (7)$$

In the case of  $\pi^-p$  collisions, the fluctuations of the  $|\overline{u}dc\overline{c}\rangle$  state produces charmed hadrons at  $x_F > 0$  in the center of mass while the fluctuations of the  $|uudc\overline{c}\rangle$  state

produces charmed hadrons at  $x_F < 0$ .

### 3.1 Single charmed hadrons

There are two ways of producing charmed hadrons from intrinsic  $c\bar{c}$  states. The first is by uncorrelated fragmentation, discussed in Section 2. Additionally, if the projectile has the corresponding valence quarks, the charmed quark can also hadronize by coalescence with the valence spectators. The coalescence mechanism thus introduces flavor correlations between the projectile and the final-state hadrons, producing *e.g.*  $D^-$ 's with a large fraction of the  $\pi^-$  momentum. In the pion fragmentation region,  $x_F > 0$ ,  $D^-$  and  $D^0$  have contributions from both coalescence and fragmentation while  $D^+$  and  $\bar{D}^0$  can only be produced from the minimal  $c\bar{c}$  Fock state by fragmentation. In the proton fragmentation region,  $x_F < 0$ , the  $D^-$  and  $\bar{D}^0$  may be produced by both coalescence and fragmentation.

If we assume that the  $c$  quark fragments into a  $D$  meson, the  $D$  distribution is

$$\frac{dP_{ic}^F}{dx_D} = \int dz \prod_{i=1}^n dx_i \frac{dP_{ic}}{dx_1 \dots dx_n} D_{D/c}(z) \delta(x_D - zx_c) , \quad (8)$$

where  $n = 4, 5$  for pion and proton projectiles in the  $|n_V c\bar{c}\rangle$  configuration. This mechanism produces  $D$  mesons carrying 25-30% of the projectile momentum with the delta function and 17-20% with the Peterson function. The  $D$  distributions are shown in Fig. 3(a) and 3(b) for proton and pion projectiles normalized to the total probability of the  $|n_V c\bar{c}\rangle$  Fock state configuration assuming that  $P_{ic}$  is the same for protons and pions. Less momentum is given to the charmed quarks in the proton than in the pion because the total momentum is distributed among more partons. These distributions are assumed for all intrinsic charm production by uncorrelated fragmentation.

The coalescence distributions, on the other hand, are specific for the individual

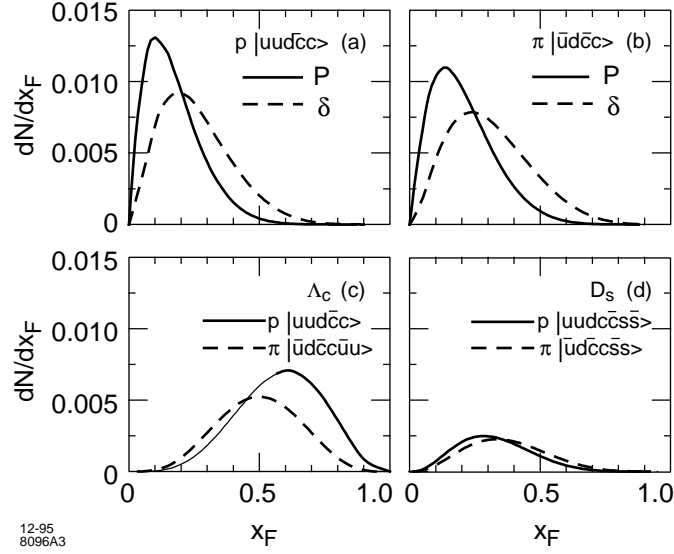


Figure 3: Charmed particle distributions from the intrinsic charm model. The charmed quark fragmentation distributions are shown for Peterson function (solid) and delta function (dashed) fragmentation for proton (a) and pion (b) projectiles. Charmed hadrons produced by coalescence from protons (solid) and pions (dashed) are also shown for (c)  $\Lambda_c$  baryons and (d)  $D_s$  mesons. The charmed quark distributions in (a) and (b) and the  $\Lambda_c$  distribution from a proton (c) are normalized to  $P_{ic}$ . The  $\Lambda_c$  distribution from a pion (c) and the  $D_s$  distributions (d) are normalized to  $P_{icu}$  and  $P_{ics}$  respectively.

charmed hadrons. The coalescence contribution to leading  $D$  production is

$$\frac{dP_{\text{ic}}^C}{dx_D} = \int \prod_{i=1}^n dx_i \frac{dP_{\text{ic}}}{dx_1 \dots dx_n} \delta(x_D - x_c - x_1) . \quad (9)$$

With the additional momentum of the light valence quark, the  $D$  takes 40-50% of the momentum. In the proton fragmentation region, the  $c$  quark can coalesce with valence  $u$  and  $d$  quarks to produce leading  $\Lambda_c$ 's,

$$\frac{dP_{\text{ic}}^C}{dx_{\Lambda_c}} = \int \prod_{i=1}^n dx_i \frac{dP_{\text{ic}}}{dx_1 \dots dx_n} \delta(x_{\Lambda_c} - x_c - x_1 - x_2) , \quad (10)$$

carrying 60% of the proton momentum. The distribution, shown in Fig. 3(c), is also normalized to  $P_{\text{ic}}$ .

Coalescence may also occur within higher fluctuations of the intrinsic charm Fock state. For example, at  $x_F > 0$ ,  $\bar{\Lambda}_c$  and  $D_s$  can be produced by coalescence from  $|n_V c \bar{c} d \bar{d}\rangle$  and  $|n_V c \bar{c} s \bar{s}\rangle$  configurations. We previously studied  $\psi\psi$  production from  $|n_V c \bar{c} c \bar{c}\rangle$  states [37]. Assuming that all the measured  $\psi\psi$  pairs [38, 39] arise from these configurations, we can relate the  $\psi\psi$  cross section,

$$\sigma_{\text{ic}}^{\psi\psi}(hN) = f_{\psi/h}^2 \frac{P_{\text{icc}}}{P_{\text{ic}}} \sigma_{\text{ic}}(hN) , \quad (11)$$

to the double intrinsic charm production probability,  $P_{\text{icc}}$ , where  $f_{\psi/h}$  is the fraction of intrinsic  $c\bar{c}$  pairs that become  $J/\psi$ 's. The upper bound on the model,  $\sigma_{\psi\psi} = \sigma_{\text{ic}}^{\psi\psi}(\pi^- N) \approx 20$  pb [38], requires  $P_{\text{icc}} \approx 4.4\%$   $P_{\text{ic}}$  [37, 40]. This value of  $P_{\text{icc}}$  can be used to estimate the probability of light quark pairs in an intrinsic charm state. We expect that the probability of additional light quark pairs in the Fock states to be larger than  $P_{\text{icc}}$ ,

$$P_{\text{icq}} \approx \left( \frac{\widehat{m}_c}{\widehat{m}_q} \right)^2 P_{\text{icc}} , \quad (12)$$

leading to  $P_{\text{icu}} = P_{\text{icd}} \approx 70.4\%$   $P_{\text{ic}}$  and  $P_{\text{ics}} \approx 28.5\%$   $P_{\text{ic}}$ .

Then with a pion projectile at  $x_F > 0$ , the  $\bar{\Lambda}_c$  coalescence distribution from a six-particle Fock state is

$$\frac{dP_{\text{ic}}^C}{dx_{\bar{\Lambda}_c}} = \int \prod_{i=1}^n dx_i \frac{dP_{\text{ic}}}{dx_1 \dots dx_n} \delta(x_{\bar{\Lambda}_c} - x_{\bar{c}} - x_1 - x_d) , \quad (13)$$

also shown in Fig. 3(c) and normalized to  $P_{\text{icu}}$ . Since half of the quarks are needed to produce the  $\bar{\Lambda}_c$ , it carries 50% of the pion momentum. The  $D_s$  mesons arising from coalescence in the  $|n_V c \bar{c} s \bar{s}\rangle$  state,

$$\frac{dP_{\text{ic}}^C}{dx_{D_s}} = \int \prod_{i=1}^n dx_i \frac{dP_{\text{ic}}}{dx_1 \dots dx_n} \delta(x_{D_s} - x_c - x_{\bar{s}}) , \quad (14)$$

carry  $\approx 30\text{-}40\%$  of the hadron momentum, as shown in Fig. 3(d) and normalized to  $P_{\text{ics}}$ . The  $D_s$  and  $\bar{D}_s$  inherit less total momentum than the leading  $D$  since the Fock state momentum is distributed over more partons. Thus as more partons are included in the Fock state, the coalescence distributions soften and approach the fragmentation distributions, Eq. (8), eventually producing charmed hadrons with less momentum than uncorrelated fragmentation from the minimal  $c\bar{c}$  state if a sufficient number of  $q\bar{q}$  pairs are included. There is then no longer any advantage to introducing more light quark pairs into the configuration—the relative probability will decrease while the potential gain in momentum is not significant. We thus do not consider  $\bar{\Lambda}_c$  production by coalescence at  $x_F < 0$  since a minimal nine-parton Fock state is required.

### 3.2 $D\bar{D}$ pair production

In any  $|n_V c \bar{c}\rangle$  state,  $D\bar{D}$  pairs may be produced by double fragmentation, a combination of fragmentation and coalescence, or, from a pion projectile only, double coalescence. We discuss only pair production at  $x_F > 0$  so that  $|\bar{u}dc\bar{c}\rangle$  is the minimal Fock state. In the proton fragmentation region, with no valence antiquark, the leading mesons would be  $D^-(\bar{c}d)$  and  $\bar{D}^0(\bar{c}u)$ . Therefore no doubly leading  $D^-\bar{D}^0$  pairs can be produced from the five parton state: two intrinsic  $c\bar{c}$  pairs are needed, *i.e.*  $|uudc\bar{c}c\bar{c}\rangle$  states, automatically softening the effect. However, doubly leading meson-baryon pairs such as  $\Lambda_c \bar{D}^0$  and  $\Sigma_c^{++} D^-$  may be produced by coalescence in the  $|uudc\bar{c}\rangle$  state. These combinations might be interesting to study in  $pp$  interactions.



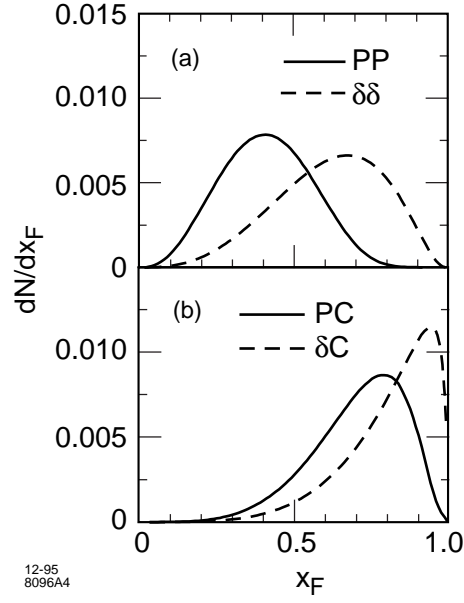


Figure 4: Intrinsic  $D\bar{D}$  distributions from a  $\pi^-$  projectile. Double fragmentation distributions are shown for Peterson function (solid) and delta function (dashed) fragmentation in (a). Charmed pairs produced by coalescence of one quark and fragmentation of the other are shown in (b) for Peterson (solid) and delta (dashed) function fragmentation. The double coalescence production from a pion is a delta function at  $x_F = 1$ . The distributions are normalized to  $P_{ic}$ .

The  $D\bar{D}$  pairs resulting from double fragmentation,

$$\begin{aligned} \frac{dP_{ic}^{FF}}{dx_{D\bar{D}}} &= \int dz_c dz_{\bar{c}} \prod_{i=1}^n dx_i \frac{dP_{ic}}{dx_1 \dots dx_n} D_{D/c}(z_c) D_{\bar{D}/\bar{c}}(z_{\bar{c}}) \\ &\times \delta(x_D - z_c x_c) \delta(x_{\bar{D}} - z_{\bar{c}} x_{\bar{c}}) \delta(x_{D\bar{D}} - x_D - x_{\bar{D}}) , \end{aligned} \quad (15)$$

carry the lowest fraction of the projectile momentum. The distributions are shown in Fig. 4(a). When both charmed quarks fragment by the Peterson function,  $\sim 40\%$  of the  $\pi^-$  momentum is given to the pair while the average is 62% with delta function fragmentation. If, *e.g.* a  $D$  is produced by coalescence while the  $\bar{D}$  is produced by fragmentation,

$$\begin{aligned} \frac{dP_{ic}^{FC}}{dx_{D\bar{D}}} &= \int dz \prod_{i=1}^n dx_i \frac{dP_{ic}}{dx_1 \dots dx_n} D_{\bar{D}/\bar{c}}(z) \\ &\times \delta(x_D - x_c - x_1) \delta(x_{\bar{D}} - z x_{\bar{c}}) \delta(x_{D\bar{D}} - x_D - x_{\bar{D}}) . \end{aligned} \quad (16)$$

These distributions, with rather large momentum fractions, 71% for Peterson fragmentation and 87% for the delta function, are shown in Fig. 4(b). When the projectile has a valence antiquark, as in the pion,  $D\bar{D}$  pair production by double coalescence is possible,

$$\frac{dP_{ic}^{CC}}{dx_{D\bar{D}}} = \int \prod_{i=1}^n dx_i \frac{dP_{ic}}{dx_1 \dots dx_n} \delta(x_D - x_c - x_1) \delta(x_{\bar{D}} - x_{\bar{c}} - x_2) \delta(x_{D\bar{D}} - x_D - x_{\bar{D}}) . \quad (17)$$

All of the momentum of the four-particle Fock state is transferred to the  $D\bar{D}$  pair, *i.e.*  $x_{D\bar{D}} \equiv 1$ . We also consider double coalescence from a pion in a six particle Fock state. In this case, 74% of the pion momentum is given to the pair, similar to the result for Peterson fragmentation with coalescence, Eq. (16), as could be expected from our discussion of  $D_s$  production in this model.

#### 4. Predictions of the Two-Component Model

We now turn to specific predictions of the  $x_F$  distributions and asymmetries in our model. The  $x_F$  distribution is the sum of the leading-twist fusion and intrinsic

charm components,

$$\frac{d\sigma}{dx_F} = \frac{d\sigma_{\text{lt}}}{dx_F} + \frac{d\sigma_{\text{ic}}}{dx_F}, \quad (18)$$

where  $d\sigma_{\text{ic}}/dx_F$  is related to  $dP_{\text{ic}}/dx_F$  in Eq. (7). Note that when we discuss uncorrelated fragmentation, the same function, either the delta or Peterson function, is used for both leading twist fusion and intrinsic charm. The intrinsic charm model produces charmed hadrons by a mixture of uncorrelated fragmentation and coalescence [12, 18]. Coalescence in the intrinsic charm model is taken to enhance the leading charm probability over nonleading charm. Since we have not made any assumptions about how the charmed quarks are distributed into the final-state charmed hadron channels, an enhancement by coalescence is not excluded as long as the total probability of all charmed hadron production by intrinsic charm does not exceed  $P_{\text{ic}}$ . Because little experimental guidance is available to help us separate the charm production channels, we have not directly addressed the issue here. Thus the above distributions are normalized to the total  $c\bar{c}$  cross section for the pair distributions and to the single charm cross section for the single charmed hadrons. This is naturally an overestimate of the cross sections in the charm channels, but more complete measurements are needed before the relative strengths of the  $D$ ,  $\Lambda_c$ ,  $D_s$ ,  $D^*$ , *etc.* contributions to the charm cross section can be understood.

In the case of nuclear targets, the model assumes a linear  $A$  dependence for leading-twist fusion and an  $A^{0.77}$  dependence for the intrinsic charm component [34]. This  $A$  dependence is included in the calculations of the production asymmetries while the  $x_F$  distributions are given for  $\pi^-p$  interactions. The intrinsic charm contribution to the longitudinal momentum distributions is softened if the  $A$  dependence is included.

#### 4.1 Single charmed hadrons

We now consider the single charmed hadron distributions produced in  $\pi^-p$  interactions at 500 GeV over the entire  $x_F$  range. Since the production mechanisms

are somewhat different for positive and negative  $x_F$ , particularly for the  $\Lambda_c$ , we will discuss the pion and proton fragmentation regions separately.

We begin with  $\Lambda_c$  production in the proton fragmentation region, negative  $x_F$ . As we have already indicated, the  $\Lambda_c$  can be produced by coalescence from the  $|uudc\bar{c}\rangle$  configuration with an average of 60% of the center-of-mass proton momentum. The  $\bar{\Lambda}_c$  can only be produced by fragmentation from a five-particle Fock state and, if a nine-particle Fock state is considered, the coalescence distribution will not be significantly harder than the fragmentation distribution shown in Fig. 3(a) since four additional light quarks are included in the minimal proton Fock state.

Therefore coalescence is only important for the  $\Lambda_c$ , leading naturally to an asymmetry between  $\Lambda_c$  and  $\bar{\Lambda}_c$ . We will assume that the same number of  $\Lambda_c$  and  $\bar{\Lambda}_c$  are produced by fragmentation and that any excess of  $\Lambda_c$  production is solely due to coalescence. Then, at  $x_F < 0$ ,

$$\frac{dP_{\text{ic}}^{\bar{\Lambda}_c}}{dx_{\bar{\Lambda}_c}} = \frac{dP_{\text{ic}}^F}{dx_{\bar{\Lambda}_c}} \quad (19)$$

$$\frac{dP_{\text{ic}}^{\Lambda_c}}{dx_{\Lambda_c}} = \frac{dP_{\text{ic}}^F}{dx_{\Lambda_c}} + r \frac{dP_{\text{ic}}^C}{dx_{\Lambda_c}}. \quad (20)$$

The fragmentation distribution is taken from Eq. (8), the coalescence distribution from Eq. (10). The parameter  $r$  is related to the integrated ratio of  $\Lambda_c$  to  $\bar{\Lambda}_c$  production. We have assumed three values of  $r$ : 1, 10, and, as an extreme case, 100. The results for the two uncorrelated fragmentation functions are shown in Fig. 5(a) and 5(b). Intrinsic charm fragmentation produces a slight broadening of the  $\bar{\Lambda}_c$  distribution for delta function fragmentation over leading-twist fusion (increasing to a shoulder for the Peterson function). The  $\Lambda_c$  distribution, strongly dependent on  $r$ , is considerably broadened.

The value  $r = 1$  is compatible with early low statistics measurements of charmed baryon production [41] where equal numbers of  $\Lambda_c$  and  $\bar{\Lambda}_c$  were found in the range

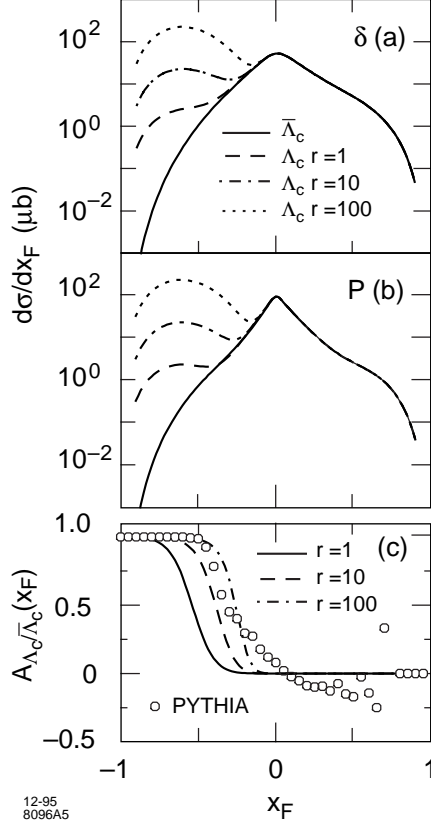


Figure 5: The  $\Lambda_c/\bar{\Lambda}_c$   $x_F$  distributions predicted by the two-component model in (a) and (b) for delta and Peterson function fragmentation respectively. The associated asymmetry is shown in (c). The  $x_F$  distributions are normalized to our calculated cross section, Eq. (18). In (a) and (b), the solid curve is the  $\bar{\Lambda}_c$  distribution (identical to  $\Lambda_c$  for  $x_F > 0$ ) while the dashed, dot-dashed, and dotted curves show  $\Lambda_c$  distributions with  $r = 1, 10$ , and  $100$ . The predicted model asymmetry for  $r = 1$  (solid),  $10$  (dashed), and  $100$  (dot-dashed) is compared with that from PYTHIA (open circles) in (c). At  $x_F > 0$ , our model predicts no asymmetry.

$|x_F| < 0.3$ . The data is often parameterized as  $(1 - |x_F|)^{n_{\Lambda_c}}$ , where

$$n_{\Lambda_c} = \frac{1 - |x_{F,\min}|}{\langle |x_F| \rangle - |x_{F,\min}|} - 2. \quad (21)$$

For  $x_F < 0$ , we predict  $n_{\Lambda_c} = 4.6$  for the delta function and 7.3 for the Peterson function. The difference is due to the steeper slope of the fusion model with the Peterson function. We find rather large values of  $n_{\Lambda_c}$  since the average  $x_F$  is dominated by the leading-twist fusion component at low  $x_F$ . If we restrict the integration to  $x_F < -0.5$ , then  $n_{\Lambda_c}$  decreases to 1.4 independent of the fragmentation mechanism<sup>†</sup>. The data on  $\Lambda_c$  production measured in  $pp$  collisions at the ISR with  $\sqrt{s} = 63$  GeV are consistent with this prediction. For  $x_F > 0.5$ ,  $n_{\Lambda_c} = 2.1 \pm 0.3$  was found [6] while for  $x_F > 0.35$ ,  $n_{\Lambda_c} = 2.4 \pm 1.3$  [7]. Hard charmed baryon distributions have also been observed at large  $x_F$  in  $nN$  interactions at the Serpukhov spectrometer with an average neutron energy of 70 GeV,  $n_{\Lambda_c} = 1.5 \pm 0.5$  for  $x_F > 0.5$  [8]. Charmed hyperons  $\Xi_c(usc)$  produced by a 640 GeV neutron beam [42] do not exhibit a strong leading behavior,  $n_{\Xi_c} = 4.7 \pm 2.3$ . This is similar to the delta function prediction for  $n_{\Lambda_c}$  when  $x_F < 0$ . On the other hand, charmed hyperons produced with a  $\Sigma^-(dds)$  beam [10, 11] are leading with  $n_{\Xi_c} = 1.7 \pm 0.7$  for  $x_F > 0.6$  [10]. Thus in the proton fragmentation region  $r = 1$  is compatible with the shape of the previously measured  $\Lambda_c$   $x_F$  distributions. When we compare the  $\Lambda_c$  cross section in the proton fragmentation region with that of leading-twist fusion, the coalescence mechanism increases the cross section by a factor of 1.4-1.7 over the fusion cross section and by 30% over the  $\bar{\Lambda}_c$  cross section.

The extreme value,  $r = 100$ , was chosen to fit the forward  $\Lambda_c$  production cross section measured at the ISR,  $B\sigma_{pp \rightarrow \Lambda_c X} = 2.84 \pm 0.5 \mu\text{b}$  [6], assuming that the charmed quark and  $\Lambda_c$  cross sections are equal, already an obvious overestimate. This choice produces a secondary peak in the  $\pi^-p$  distributions at  $x_F \sim -0.6$ , the average  $\Lambda_c$

---

<sup>†</sup>The parameterization  $(1 - x_F)^n$  is only good if the distribution is monotonic. However, our two-component  $\Lambda_c$  distribution does not fit this parameterization over all  $x_F$ . At low  $x_F$ , the leading-twist component dominates. If only the high  $x_F$  part is included, the value of  $\langle |x_F| \rangle$  is a more accurate reflection of the shape of the intrinsic charm component.

momentum from coalescence. Such a large value of  $r$  implies that the intrinsic charm cross section is considerably larger than the leading-twist cross section.

The shape of the distribution with  $r = 100$  is similar to that due to diquark coalescence in PYTHIA [19], shown in Fig. 1(c), except that the PYTHIA distribution peaks at  $x_F \approx -0.9$  due to the acceleration induced by the string mechanism. While a measurement of the  $\Lambda_c$  cross section over the full phase space in the proton fragmentation region is lacking, especially for  $pp$  interactions at  $x_F > 0$ , no previous measurement shows an increase in the  $\Lambda_c$   $x_F$  distributions as implied by these results. However, the reported  $\Lambda_c$  production cross sections are relatively large [6, 7, 8, 42], between  $40 \mu\text{b}$  and  $1 \text{ mb}$  for  $10 \leq \sqrt{s} \leq 63 \text{ GeV}$ . In particular, the low energy cross sections are much larger than those reported for the  $c\bar{c}$  total cross section at the same energy. This is not yet understood.

A few remarks are in order here. Some of these experiments [7, 8] extract the total cross section by extrapolating flat forward  $x_F$  distributions back to  $x_F = 0$  and also assume associated production, requiring a model of  $\bar{D}$  production. On the other hand, the reported  $c\bar{c}$  total cross sections are usually extracted from  $D$  measurements at low to moderate  $x_F$  and would therefore hide any important coalescence contribution to charmed baryon production at large  $x_F$ . High statistics measurements of charmed mesons and baryons over the full forward phase space ( $x_F > 0$ ) in  $pp$  interactions would help resolve both the importance of coalescence and the magnitude of the total  $c\bar{c}$  production cross section.

We also chose  $r = 10$  as an intermediate value. In this case, a secondary peak is also predicted but the cross section at  $x_F < 0$  is only a factor of two to three larger than the fusion cross section rather than the factor of 21 needed to fit the ISR data at  $x_F > 0.5$ . The magnitude of the second maximum is also less than the fusion cross section in the central region.

An important test of the production mechanism for charm hadroproduction is the

$\Lambda_c$  and  $\bar{\Lambda}_c$  asymmetry, defined as

$$\mathcal{A}_{\Lambda_c/\bar{\Lambda}_c} = \frac{d\sigma(\Lambda_c) - d\sigma(\bar{\Lambda}_c)}{d\sigma(\Lambda_c) + d\sigma(\bar{\Lambda}_c)} . \quad (22)$$

If  $\mathcal{A}_{\Lambda_c/\bar{\Lambda}_c}$  is assumed to arise only from initial state coalescence, we can estimate the parameter  $r$  from the E791 500 GeV  $\pi^- A$  data. Our calculated asymmetries for the three  $r$  values<sup>‡</sup> are compared with the results from PYTHIA in Fig. 5(c). It is, as expected, closest to our model with  $r = 100$  although the asymmetry predicted by PYTHIA does not increase as abruptly as in our model.

Preliminary data from E791 [43] indicate a significant asymmetry for  $x_F$  as small as  $-0.1$ , albeit with large uncertainty. The intrinsic charm model in its simplest form can only produce such asymmetries if  $r \geq 100$ , against intuition. Alternatively, a softer  $\Lambda_c$  distribution from coalescence would make a larger asymmetry at lower  $|x_F|$ , thus allowing a smaller  $r$ . Such a softening could be due to either an important contribution to  $\Lambda_c$  production from a  $|n_V gc\bar{c}\rangle$  configuration or a different assumption about the  $|n_V c\bar{c}\rangle$  wavefunction [44]. In a more realistic model, both initial and final state coalescence will play some role in  $\Lambda_c$  production. Final-state coalescence, added to the leading-twist fusion prediction, would also require a smaller  $r$ .

At  $x_F > 0$  there is no asymmetry in  $\pi^- p$  interactions since both the baryon and antibaryon can be produced by fragmentation from a  $|\bar{u}dc\bar{c}\rangle$  state and by coalescence from a  $|\bar{u}dc\bar{c}q\bar{q}\rangle$  state ( $q = u, d$ ). Then

$$\frac{dP_{\text{ic}}^{\Lambda_c}}{dx_{\Lambda_c}} = \frac{dP_{\text{ic}}^{\bar{\Lambda}_c}}{dx_{\bar{\Lambda}_c}} = \frac{dP_{\text{ic}}^F}{dx_{\Lambda_c}} + \frac{P_{\text{icq}}}{P_{\text{ic}}} \frac{dP_{\text{ic}}^C}{dx_{\Lambda_c}} . \quad (23)$$

The coalescence contribution, obtained from Eq. (13), produces a small shoulder in the distributions at  $x_F > 0$ . We extract  $n_{\Lambda_c} = 4.1$  for  $x_{F,\text{min}} = 0$ , in good agreement with the NA32 measurement,  $n_{\Lambda_c} = 3.5 \pm 0.5$  [27]. The same mechanism can account for both  $\Lambda_c$  and  $\bar{\Lambda}_c$  production in the  $\pi^-$  fragmentation region since no asymmetry is observed [43], which is also in accord with the NA32 result,  $\sigma(\Lambda_c)/\sigma(\bar{\Lambda}_c) \approx 1$  [27].

---

<sup>‡</sup>We have only shown the delta function results. Those with the Peterson function are quite similar. The slope increases slightly but the point where  $\mathcal{A}_{\Lambda_c/\bar{\Lambda}_c} > 0$  does not shift.



To look for subtle coalescence effects as well as to understand the large difference between  $\Lambda_c$  and  $\bar{\Lambda}_c$  production at  $x_F \approx -0.1$  it is important to compare the shape of the momentum distributions in addition to the asymmetries.

Assuming that equal numbers of  $D_s$  and  $\bar{D}_s$  are produced, the  $x_F$  distributions are

$$\frac{dP_{\text{ic}}^{D_s}}{dx_{D_s}} = \frac{dP_{\text{ic}}^{\bar{D}_s}}{dx_{\bar{D}_s}} = \frac{dP_{\text{ic}}^F}{dx_{D_s}} + \frac{P_{\text{ics}}}{P_{\text{ic}}} \frac{dP_{\text{ic}}^C}{dx_{D_s}}. \quad (24)$$

The coalescence contribution is given by Eq. (14) and the distributions are shown in Fig. 6. The shoulder at  $x_F > 0$  predicted in charmed baryon production is absent for  $D_s$  production. Coalescence does not produce a significant enhancement of  $D_s$ 's since  $P_{\text{ics}} < P_{\text{icu}}$ . The average momentum gain over uncorrelated fragmentation of the  $|n_V c \bar{c}\rangle$  state is small. The forward distributions in Fig. 6 are only slightly harder than those from leading-twist production. This is also true for  $x_F < 0$  where the  $D_s$ ,  $\bar{D}_s$  distributions are not significantly different from the  $\bar{\Lambda}_c$  distributions even though coalescence is included in the production of the  $D_s$  and not in  $\bar{\Lambda}_c$ . When we compare our distribution with the parameterization  $(1-x_F)^{n_{D_s}}$ , we extract  $n_{D_s} = 4.7$  at  $x_F > 0$ , in agreement with the NA32 measurement,  $n_{D_s} = 3.9 \pm 0.9$  [27].

We find  $\mathcal{A}_{D_s/\bar{D}_s}(x_F) = 0$  for all  $x_F$  in our model since the production mechanisms are everywhere identical for the particle and antiparticle. In contrast to the intrinsic charm model, the  $D_s$  excess predicted by PYTHIA in the proton region, shown in Fig. 1(d), leads to a backward asymmetry similar to  $\mathcal{A}_{\Lambda_c/\bar{\Lambda}_c}$ , shown in Fig. 6(c).

## 4.2 $D\bar{D}$ production

We simplify our discussion of  $D\bar{D}$  pair production by several respects. We have assumed that equal numbers of  $D^*$  mesons and, separately, primary  $D$  mesons are produced by fragmentation and that any production excess is the result of coalescence. Thus the  $D\bar{D}$  and  $D^*\bar{D}^*$   $x_F$  distributions are equivalent within the model and the analysis applies for both types of pairs unless stated otherwise. Therefore we shall

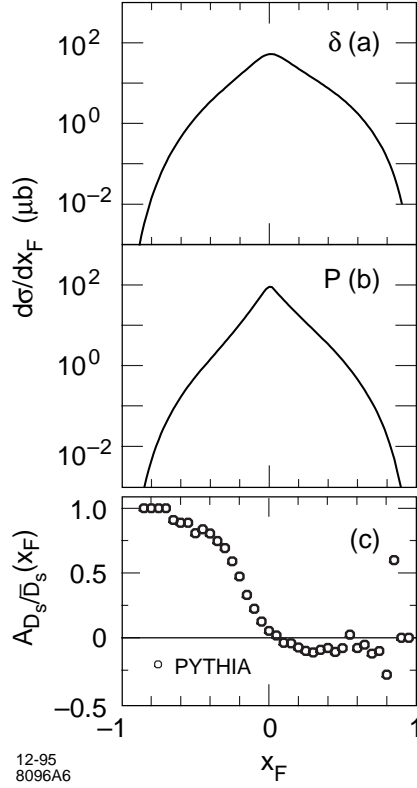


Figure 6: The  $D_s/\overline{D}_s$   $x_F$  distributions predicted by the two-component model in (a) and (b) for delta and Peterson function fragmentation respectively. The associated asymmetry from our model and PYTHIA (open circles) is shown in (c). Our model predicts no asymmetry.

also implicitly assume that all secondary  $D$ 's produced by  $D^*$  decays can be separated from the primary  $D$ 's. We do not consider  $D\overline{D}^*$  or  $D^*\overline{D}$  pairs.

We use the same pair classification as in our discussion of the pair distributions from PYTHIA, shown in Fig. 2(c) and 2(d). Then the probability distributions for intrinsic charm pair production are:

$$\frac{dP_{\text{ic}}^{NN}}{dx_{D\overline{D}}} = \frac{dP_{\text{ic}}^{FF}}{dx_{D\overline{D}}} \quad (25)$$

$$\frac{dP_{\text{ic}}^{NL}}{dx_{D\overline{D}}} = 2 \left( \frac{dP_{\text{ic}}^{FF}}{dx_{D\overline{D}}} + 1.2 \frac{dP_{\text{ic}}^{FC}}{dx_{D\overline{D}}} \right) \quad (26)$$

$$\frac{dP_{\text{ic}}^{LL}}{dx_{D\overline{D}}} = \frac{dP_{\text{ic}}^{FF}}{dx_{D\overline{D}}} + 1.2 \left( \frac{dP_{\text{ic}}^{FC}}{dx_{D\overline{D}}} + P_{\text{ic}}^{CC} \delta(x_{D\overline{D}} - 1) + \frac{P_{\text{icq}}}{P_{\text{ic}}} \frac{dP_{\text{ic}}^{CC}}{dx_{D\overline{D}}} \right) . \quad (27)$$

In the above, we have assumed that there is a 20% production enhancement due to coalescence, *e.g.*

$$\frac{dP_{\text{ic}}^{D^-}}{dx_{D^-}} = \frac{dP_{\text{ic}}^F}{dx_{D^-}} + 1.2 \frac{dP_{\text{ic}}^C}{dx_{D^-}} . \quad (28)$$

This assumption is different from our calculation of  $\mathcal{A}_{D^-/D^+}$  in [12] where we assumed that the  $D^-$  and  $D^+$  production probabilities were equal even though the  $D^-$  is produced by coalescence and the  $D^+$  is not. This resulted in a small negative asymmetry at low  $x_F$ . When  $\mathcal{A}_{D^-/D^+}$  is recalculated with the  $D^-$  distribution in Eq. (28), the model asymmetry is never negative and better agreement with the data [1, 4, 5] is found.

A factor of two has been included in the  $NL$  distribution because there are two sources of the  $NL$  pairs ( $D^-D^+$  and  $D^0\overline{D}^0$ ) relative to the  $LL$  and  $NN$  pairs. This factor is also included in the leading-twist production cross section. The last term in the  $LL$  distribution, from the six-particle Fock state, is the only significant source of pairs due to double coalescence, causing the  $LL$  distributions to be somewhat harder than the  $NL$  distributions. The pair distributions are given in Fig. 7(a) and 7(b). Note that even the  $NN$  distribution with the Peterson function in Fig. 7(b) is broadened considerably over the leading twist distribution shown in Fig. 2(b). The

predicted slopes of the pair distributions from the various sources begin to differ for  $x_F > 0.25$ .

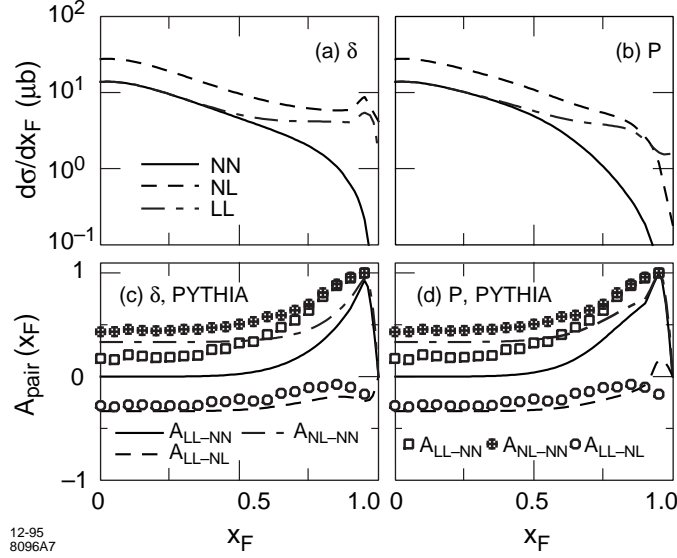


Figure 7: The  $D\bar{D}$  pair distributions from  $\pi^-p$  interactions at 500 GeV for  $NN$  (solid),  $NL$  (dashed), and  $LL$  (dot-dashed) pairs are shown in (a) and (b) for delta function and Peterson function fragmentation. The intrinsic charm model distributions are given in Eqs. (25)-(27). The asymmetries for delta function and Peterson function fragmentation from the two-component model, calculated using Eqs. (29)-(31), are shown in (c) and (d). They are compared with the  $D^*\bar{D}^*$  asymmetries from PYTHIA for  $\mathcal{A}_{LL-NN}$  (solid curve and squares),  $\mathcal{A}_{LL-NL}$  (dashed curve and circles), and  $\mathcal{A}_{NL-NN}$  (dot-dashed curve and crosses).

We define the following three asymmetries:

$$\mathcal{A}_{LL-NN} = \frac{d\sigma(LL) - d\sigma(NN)}{d\sigma(LL) + d\sigma(NN)} \quad (29)$$

$$\mathcal{A}_{LL-NL} = \frac{d\sigma(LL) - d\sigma(NL)}{d\sigma(LL) + d\sigma(NL)} \quad (30)$$

$$\mathcal{A}_{NL-NN} = \frac{d\sigma(NL) - d\sigma(NN)}{d\sigma(NL) + d\sigma(NN)}, \quad (31)$$

shown in Fig. 7(c) and 7(d) for delta and Peterson function fragmentation. The corresponding  $D^*\bar{D}^*$  asymmetries from PYTHIA are also shown since the leading assignments are unaffected by decays. It is interesting to study all three asymmetries.

Since twice as many  $NL$  pairs are produced by definition,  $\mathcal{A}_{LL-NL}$  is negative for all  $x_F$ . The change in  $\mathcal{A}_{LL-NL}$  at  $x_F \sim 1$  in Fig. 7(d) is due to double coalescence from the  $|\bar{u}dc\bar{c}\rangle$  state. Larger values of  $\mathcal{A}_{NL-NN}$  and  $\mathcal{A}_{LL-NN}$  are predicted by PYTHIA than by our model due to our different assumptions about particle production. However, the general trends are quite similar for the final-state coalescence mechanism of PYTHIA and the initial-state coalescence of our model. This is perhaps not surprising since the single  $D$  asymmetries from the two models would be quite similar if the same assumptions were made about the initial production ratios at  $x_F = 0$ .

## 5. Conclusions

We have studied single charmed hadron and charmed meson pair longitudinal momentum distributions and the related asymmetries within the intrinsic charm model and PYTHIA. In conventional leading-twist perturbative QCD, there is no asymmetry between charmed and anticharmed hadrons. In the intrinsic charm model as well as in PYTHIA, the asymmetry is clearly due to coalescence. However, we find that the asymmetries alone cannot tell the full story, especially at  $x_F > 0$ . The individual  $x_F$  distributions are needed over all  $x_F$  to unravel the production properties of the charmed hadrons since only the shapes of these distributions can reveal deviations from the fusion predictions.

The  $D\bar{D}$  pair asymmetries are also quite interesting, particularly at high pair momentum. We have not considered their production at negative  $x_F$  in this paper due to the ambiguity in leading particle assignments. However, since only  $D^-$  or  $\bar{D}^0$  can be produced by coalescence from the five-particle Fock state, a study of  $\Lambda_c\bar{D}^0$  or  $\Sigma_c D^-$  pairs could prove more enlightening.

Given our  $\Lambda_c$  predictions at  $x_F < 0$  in  $\pi^- p$  interactions, it would be quite interesting if high statistics measurements of  $\Lambda_c$  production can be made in  $pp$  collisions at  $|x_F| > 0$  to clarify charmed baryon production. Since we would predict similar

behavior for bottom hadron production, such studies would also be of interest. Although a rise in  $d\sigma/dx_F$  with  $x_F$  seems counterintuitive, such distributions have been observed in diffractive  $\Xi^-$  and  $\Omega^-$  production in  $\Xi^-$ -Be interactions [45]. Studies of charmed baryon production by a hyperon beam within the context of this model are underway.

### Acknowledgments

We would like to thank J. A. Appel, T. Carter, W. Geist, P. Hoyer, J. Leslie, S. Kwan, M. Moinster, A. Mueller, E. Quack, T. Sjöstrand, and W.-K. Tang for discussions. This work was supported in part by the Director, Office of Energy Research, Division of Nuclear Physics of the Office of High Energy and Nuclear Physics of the U. S. Department of Energy under Contract No. DE-AC03-76SF0098 and DE-AC03-76SF00515.

## References

- [1] T. Carter, in proceedings of *DPF '94*, the 8<sup>th</sup> meeting of the APS Division of Particles and Fields, Albuquerque, NM, 1994, S. Seidel ed.
- [2] M. Aguilar-Benitez *et al.*, Phys. Lett. **161B** (1985) 400, Z. Phys. **C31** (1986) 491.
- [3] S. Barlag *et al.*, Z. Phys. **C49** (1991) 555.
- [4] M. Adamovich *et al.*, Phys. Lett. **B305** (1993) 402.
- [5] G.A. Alves *et al.*, Phys. Rev. Lett. **72** (1994) 812.
- [6] P. Chauvat *et al.*, Phys. Lett. **199B** (1987) 304 and references cited therein.
- [7] G. Bari *et al.*, Nuovo Cimento **104A** (1991) 57.
- [8] A.N. Aleev *et al.*, Z. Phys. **C23** (1984) 333.
- [9] G. Bari *et al.*, Nuovo Cimento **104A** (1991) 787.
- [10] S.F. Biagi *et al.*, Z. Phys. **C28** (1985) 175.
- [11] R. Werding, WA89 Collaboration, in proceedings of ICHEP94, Glasgow.
- [12] R. Vogt and S.J. Brodsky, Nucl. Phys. **B438** (1995) 261.
- [13] J.C. Collins, D.E. Soper and G. Sterman, *Perturbative QCD*, ed. A. H. Mueller (World Scientific, Singapore, 1989). G. Bodwin, Phys. Rev. **D31** (1985) 2616, **D34** (1986) 3932. J. Qiu and G. Sterman, Nucl. Phys. **B353** (1991) 105,137.
- [14] S.J. Brodsky, J. Gunion. D. Soper, Phys. Rev. **D36** (1987) 2710.
- [15] S.J. Brodsky, P. Hoyer, C. Peterson and N. Sakai, Phys. Lett. **B93** (1980) 451; S. J. Brodsky, C. Peterson and N. Sakai, Phys. Rev. **D23** (1981) 2745.

- [16] S.J. Brodsky, P. Hoyer, A.H. Mueller and W.-K. Tang, Nucl. Phys. **B369** (1992) 519.
- [17] R. Vogt, S.J. Brodsky and P. Hoyer, Nucl. Phys. **B360** (1991) 67.
- [18] R. Vogt, S.J. Brodsky and P. Hoyer, Nucl. Phys. **B383** (1992) 643.
- [19] T. Sjöstrand, Comput. Phys. Commun. **39** (1986) 347. T. Sjöstrand and M. Bengtsson, Comput. Phys. Commun. **43** (1987) 367.
- [20] R. Vogt, LBL preprint, LBL-37105, to be published in Z. Phys. **C**.
- [21] S. Frixione, M. L. Mangano, P. Nason, and G. Ridolfi, Nucl. Phys. **B431** (1994) 453.
- [22] M. Glück, E. Reya, and A. Vogt, Z. Phys. **C53** (1992) 127.
- [23] M. Glück, E. Reya, and A. Vogt, Z. Phys. **C53** (1992) 651.
- [24] C. Peterson, D. Schlatter, I. Schmitt, and P. Zerwas, Phys. Rev. **D27** (1983) 105.
- [25] M. Aguilar-Benitez *et al.*, Phys. Lett. **B189** (1987) 476.
- [26] M. Aguilar-Benitez *et al.*, Phys. Lett. **B161** (1985) 400; Z. Phys. **C31** (1986) 491.
- [27] S. Barlag *et al.*, Phys. Lett. **B247** (1990) 113.
- [28] J. Chirn, in proceedings of the ‘International Symposium on the Production and Decay of Heavy Flavors’, Stanford, CA, E. Bloom and A. Fridman Editors, (1987) 131.
- [29] R.J. Cashmore, in proceedings of the ‘International Symposium on the Production and Decay of Heavy Flavors’, Stanford, CA, E. Bloom and A. Fridman Editors, (1987) 118.



- [30] T. Sjöstrand, private communication.
- [31] V.A. Bednyakov, Mod. Phys. Lett. **A10** (1995) 61; V.G. Kartvelishvili, A.K. Likhoded, and S.R. Slobospitskii, Sov. J. Nucl. Phys. **33**(3) (1981) 434 [Yad. Fiz. **33** (1981) 832].
- [32] R.C. Hwa, Phys. Rev. **D27** (1983) 653; Phys. Rev. **D51** (1995) 85.
- [33] P. Hoyer and S.J. Brodsky, Nashville Part. Prod. 1990, p. 238.
- [34] J. Badier *et al.*, Z. Phys. **C20** (1983) 101.
- [35] J.J. Aubert *et al.*, Phys. Lett. **110B** (1982) 73; E. Hoffmann and R. Moore, Z. Phys. **C20** (1983) 71.
- [36] B.W. Harris, J. Smith, and R. Vogt, LBL-37266 and ITP-SB-95-15, to be published in Nucl. Phys. **B**.
- [37] R. Vogt and S.J. Brodsky, Phys. Lett. **B349** (1995) 569.
- [38] J. Badier *et al.*, Phys. Lett. **114B** (1982) 457.
- [39] J. Badier *et al.*, Phys. Lett. **158B** (1985) 85.
- [40] R. Vogt, Nucl. Phys. **B446**, (1995) 159.
- [41] M. Aguilar-Benitez *et al.*, Phys. Lett. **B199** (1987) 462.
- [42] J.P. Cumulat *et al.*, SLAC Summer Inst. 1987:477 (QCD161:S76:1987).
- [43] S. Kwan, E791 collaboration, private communication.
- [44] F.S. Navarra, M. Nielsen, C.A.A. Nunes and M. Teixeira, São Paulo preprint IFUSP/P-1150.
- [45] S.F. Biagi *et al.*, Z. Phys. **C34** (1987) 187.